Science Advances
AAAS

advances.sciencemag.org/cgi/content/full/7/23/eabe4206/DC1

Supplementary Materials for

Strongly enhanced and tunable photovoltaic effect in ferroelectric-paraelectric superlattices

Yeseul Yun, Lutz Mühlenbein, David S. Knoche, Andriy Lotnyk, Akash Bhatnagar*

*Corresponding author. Email: akash.bhatnagar@physik.uni-halle.de

Published 2 June 2021, *Sci. Adv.* **7**, eabe4206 (2021)
DOI: 10.1126/sciadv.abe4206

This PDF file includes:

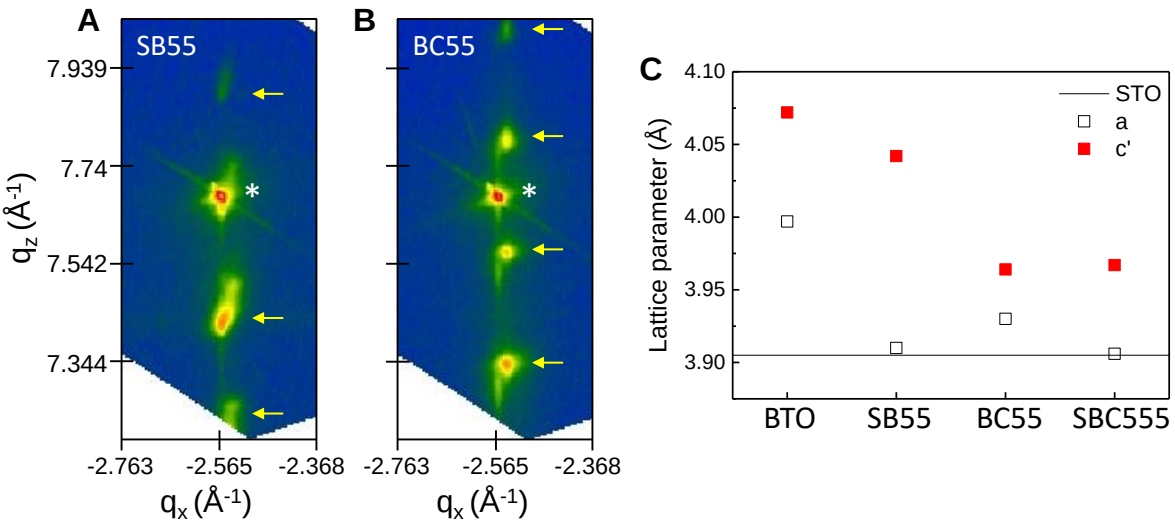

Fig. S1. Structural characterization of two-color superlattices. Reciprocal space mapping around (103) plane of (**A**) SB55 and (**B**) BC55. Star and yellow arrows indicate STO substrate and satellite peaks from SL, respectively. (**C**) Lattice parameters of single, 2- and 3-color SLs. Solid line indicates the lattice parameter of STO substrate.

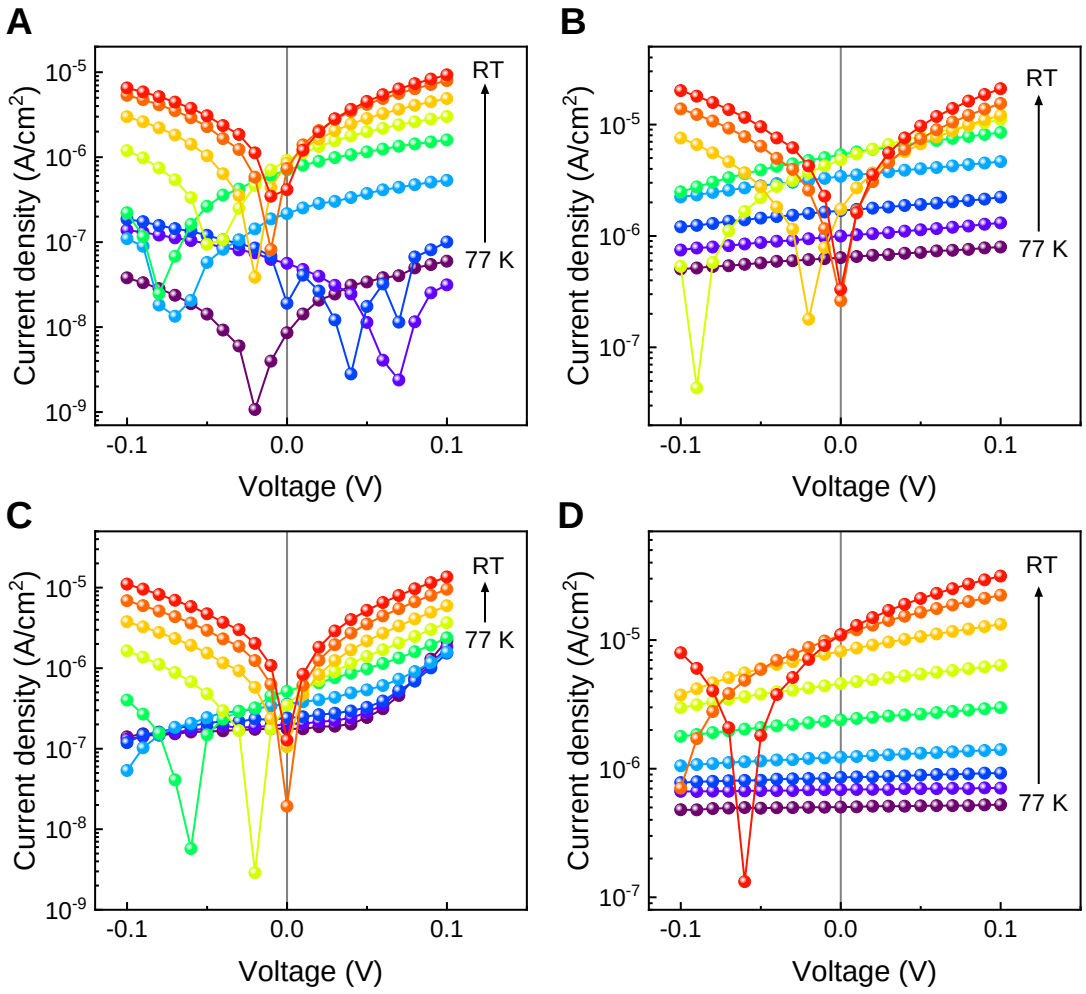

Fig. S2. Temperature dependent photo IV characteristics. Current-voltage (IV) characteristics measured with 3.06 eV of (**A**) BTO, (**B**) SB55, (**C**) BC55 and (**D**) SBC555. The dip in the IV curve represents open circuit voltage (V_{OC}). As the temperatures are lowered, the magnitude of V_{OC} gradually increases and eventually goes beyond the range of voltage used for the photoelectrical measurements. The IV curves therefore appear to be much more linear at lower temperatures.

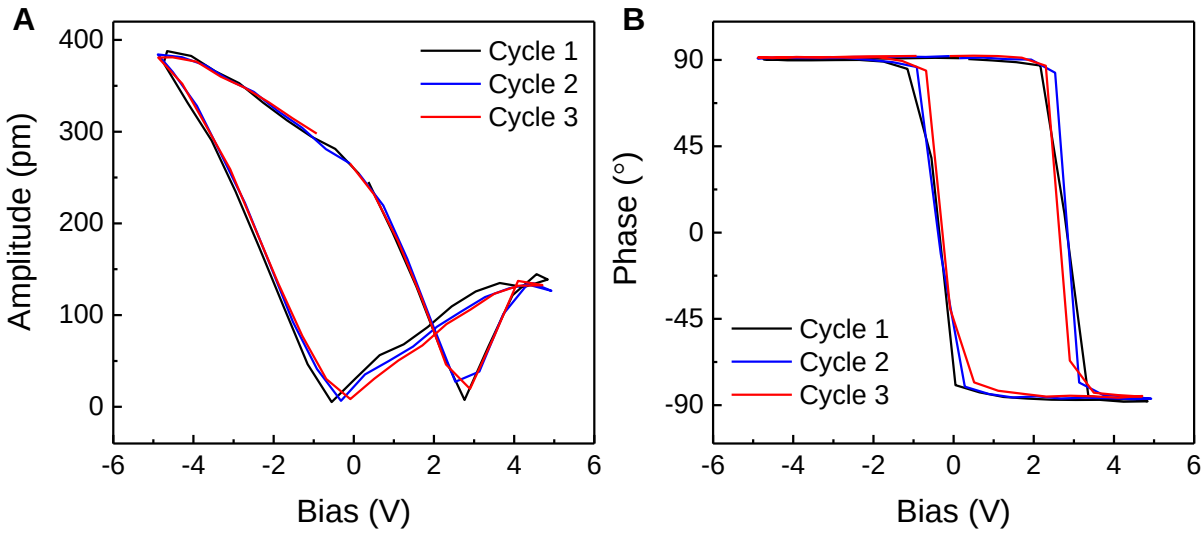

Fig. S3. Piezoresponse from superlattice. (**A**) Amplitude-Voltage and, (**B**) Phase-Voltage characteristics acquired with PFM from sample SBC222 at room temperature. The measurements were conducted with the PFM in DART (dual amplitude resonance tracking) mode.

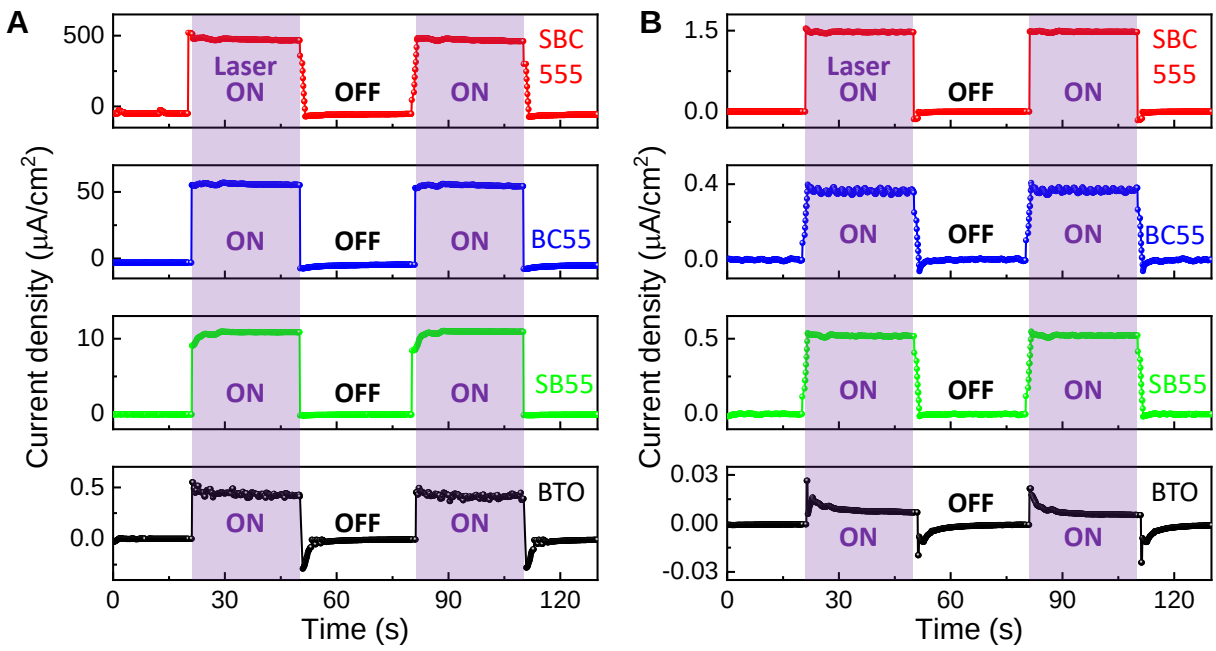

Fig. S4. Photo-response measured with time. Current-time response acquired with the illumination ON and OFF at (**A**) RT and (**B**) 77K.

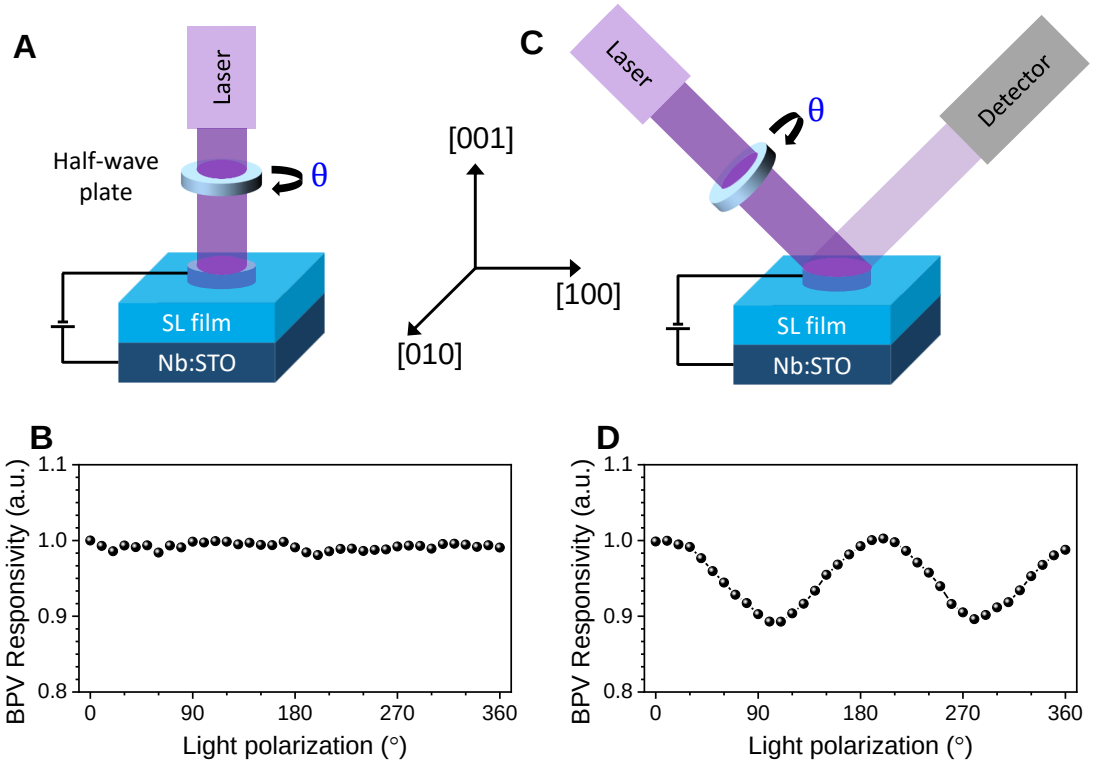

Fig. S5. The angle-dependent photovoltaic current of SBC222. (**A**) Schematic of the measurement geometry with illumination along the direction of [001] and, (**B**) the resultant BPV responsivity. The vaules are normalized to the maximum value. (**C**) Schematic of the measurement geometry with light source tilted by 45° and, (**D**) the resultant BPV responsivity. The BPV responsivity was subtracted from the obtained and normalized PV current and absorbed intensity of light.

The linear BPV current can be written as:

$$\mathbf{J}_i = I\boldsymbol{\beta}_{ijk}\mathbf{e}_j\mathbf{e}_k \tag{S1}$$

where I is the intensity of the light, $\boldsymbol{\beta}_{ijk}$ is the third-rank BPV tensor and $\mathbf{e}_j$ and $\mathbf{e}_k$ are the components of the light polarization vector. The space group of BTO is *P4mm* and

corresponding third-rank tensor is

$$\boldsymbol{\beta}_{ijk} = \begin{pmatrix} 0 & 0 & 0 & 0 & \beta_{15} & 0 \\ 0 & 0 & 0 & \beta_{15} & 0 & 0 \\ \beta_{31} & \beta_{31} & \beta_{33} & 0 & 0 & 0 \end{pmatrix} \tag{S2}$$

When the propagation direction of the incident light is along [001], the resultant BPV current will be

$$\mathbf{J}_i = I \begin{pmatrix} 0 & 0 & 0 & 0 & \beta_{15} & 0 \\ 0 & 0 & 0 & \beta_{15} & 0 & 0 \\ \beta_{31} & \beta_{31} & \beta_{33} & 0 & 0 & 0 \end{pmatrix} \begin{pmatrix} \cos^2\theta \\ \sin^2\theta \\ 0 \\ 0 \\ 0 \\ \frac{1}{2}\sin 2\theta \end{pmatrix} = I \begin{pmatrix} 0 \\ 0 \\ \beta_{31} \end{pmatrix} \tag{S3}$$

wherein θ represents the angle which light makes with the direction of current flow. It becomes apparent from the above equation that the resultant photocurrent flows only along [001] and is independent of θ, which is also consistent with the experimental result (**Fig. S5B**).

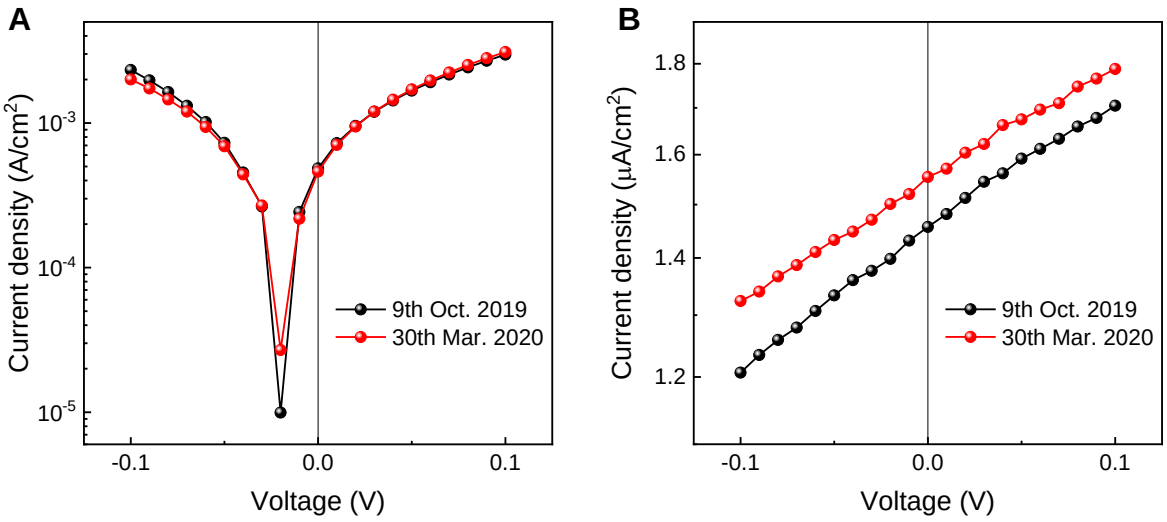

Fig. S6. Long-term photocurrent reproducibility in SBC222. IV characteristics measured with 3.06 eV at (**A**) RT and (**B**) 77K.

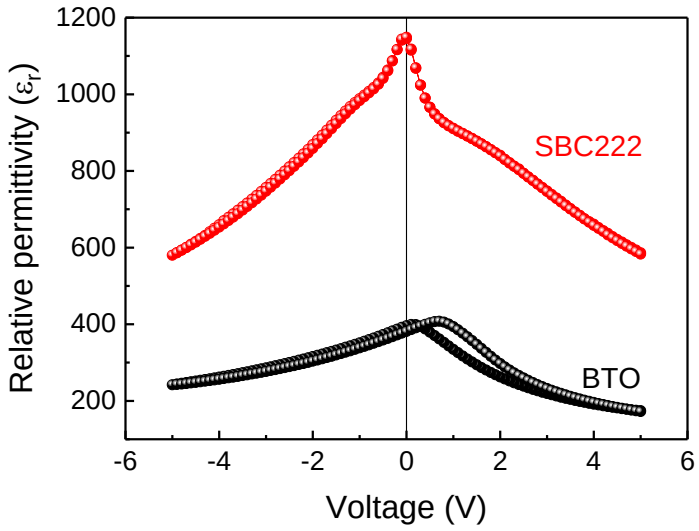

Fig. S7. Relative permittivity measured as a function of *dc* bias. The measurements are performed at 100 kHz with a 100 mV *ac* signal.

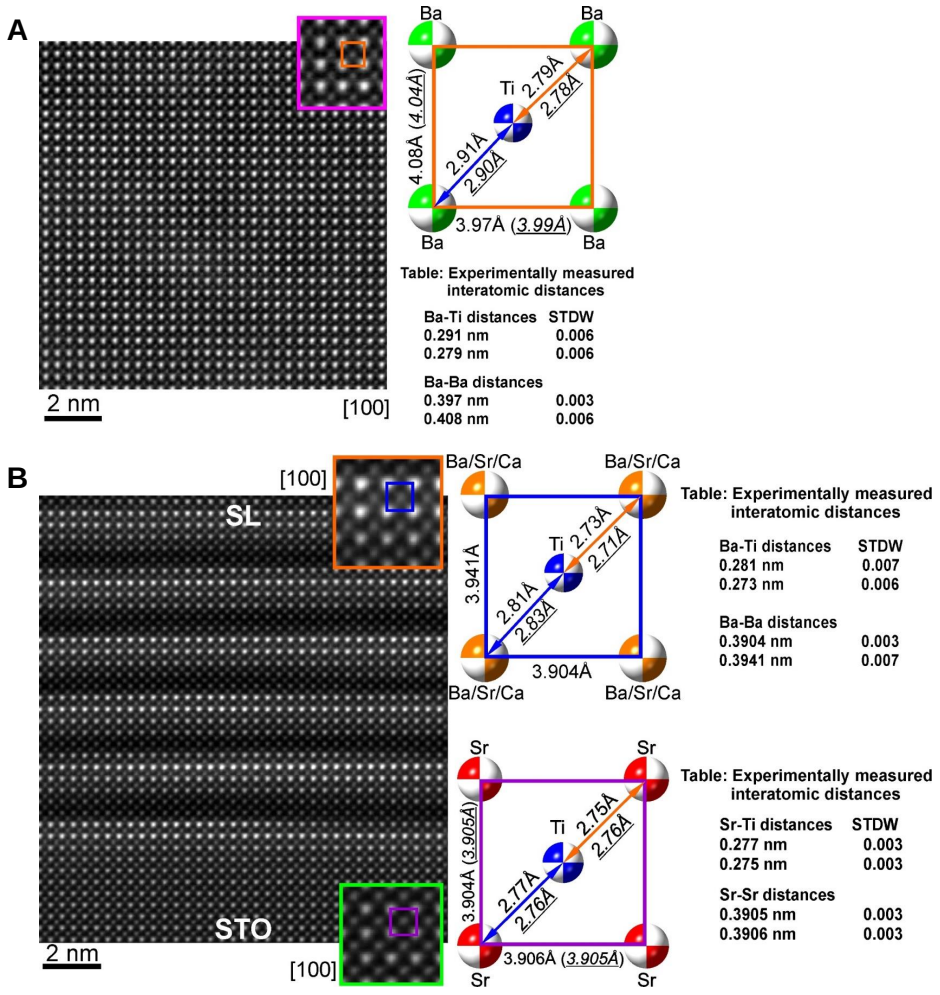

Fig. S8. Tetragonality of BTO and within superlattice. Evaluation of projected lattice distances in (**A**) BTO and (**B**) SBC222 SL. (Left) Atomic-resolution STEM-HAADF image. The inset show magnified images with unit cells marked by rectangles. (Right) Structure models derived from the experimental HADDF image. The underlined italic values show lattice distances extracted from theoretical structure. The values in table represent averaged interatomic distances calculated using at least 1000 measurement points for a particular crystallographic axis. The STDW is the standard deviation.